

## Phase diagram of multiply connected superconductors: A thin-wire loop and a thin film with a circular hole

A. Bezryadin

*Centre de Recherches sur les très Basses Températures—CNRS, B.P. 166X, 38042 Grenoble, Cedex 9, France*

A. Buzdin\*

*Service de Physique Statistique, Magnétisme et Supraconductivité—Centre d'Etude Nucléaire de Grenoble, 38054 Grenoble, Cedex 9, France*

B. Pannetier

*Centre de Recherches sur les très Basses Températures—CNRS, B.P. 166X, 38042 Grenoble, Cedex 9, France*

(Received 16 August 1994)

The phase diagram of a thin superconducting film with a circular hole in axial magnetic field is presented. The result is obtained by solving numerically the nonlinear Ginzburg-Landau (GL) equation in the limit of a thin film with large  $\kappa_{\text{eff}} = \lambda_{\text{eff}}/\xi$  (where  $\lambda_{\text{eff}} = \lambda^2/d$  is the effective screening length for a film of thickness  $d$ ). First-order phase transitions between localized (around the hole) superconducting states with different orbital momenta are predicted. Corresponding jumps in the magnetic moment, latent heat, and specific heat are presented in the universal form. The same problem is solved analytically for a thin-wire superconducting loop. All the results obtained for a film with a circular hole are valid for high- $T_c$  superconductors with columnar defects because in such compounds the GL parameter  $\kappa \sim 100$  so the screening effect is negligible: a relative distortion of the phase diagram after taking into account the screening effect is proportional to  $1/\kappa^2$  in the three-dimensional case and  $1/\kappa_{\text{eff}}$  in the case of a thin film.

### I. INTRODUCTION

Recently it has been predicted theoretically<sup>1</sup> and confirmed experimentally<sup>2</sup> that the critical field of superconducting transition near a circular hole is higher than that of a uniform sample and reveals an oscillatory temperature dependence with discontinuities in the first derivative (cusps). This behavior is due to the appearance of a localized superconducting state ( $LS_n$ ) at the hole edge characterized by a definite angular momentum  $n$  [ $n$  is integer, see (4)]. It is somewhat similar to the Little-Parks oscillations.<sup>3</sup> Such an effect may strongly influence the properties of ion-irradiated high- $T_c$  superconductors where the heavy ions create columnar defects.<sup>4,5</sup> These columnar defects cause behavior similar to the circular holes. Then the localized superconductivity might appear near the defect at the field higher than the bulk critical field. Moreover the angular momentum  $n$  is just the number of flux quanta which could be trapped by the columnar defect at lower temperature. In this context the experimental studies of the artificially prepared superconducting films with a system of regular holes<sup>2</sup> is important for better understanding of the properties of irradiated high- $T_c$  superconductors.

In Refs. 1 and 2 the primary interest has been focused on the nucleation of superconductivity [normal-state ( $N$ )  $\rightarrow$   $LS_n$  transition]. However the transitions between the localized superconducting states with different  $n$  ( $LS_n \rightarrow LS_{n+1}$ ) are possible when the magnetic field and/or the temperature changes. Such transitions are of

first order and accompanied by jumps of the magnetic moment and latent heat. It should be emphasized that different multiply connected superconducting systems (hollow cylinders,<sup>3,6</sup> loops,<sup>7</sup> networks<sup>8</sup>) were considered in many experimental and theoretical works but in most case only the transition from the normal into the superconducting state was discussed (such characteristics as critical current and magnetization were also considered but within a fixed quantum state of the system). In our paper we consider transitions between different superconducting states below the critical temperature in multiply connected systems.

In Sec. II we review the main results of Refs. 1 and 2. In Sec. III we add general formulas which are useful for the analysis of transitions between states of different orbital momentum. In Sec. IV we consider analytically a simple example: thin-wire loop (Little-Parks geometry) and analyze its phase diagram including the region below the superconducting transition. A similar problem (hollow cylinder) was considered by Fink and Grunfeld<sup>6</sup> in greater detail (taking into account the screening effect) but they discussed only the transition from the normal into the superconducting state. In Sec. V we discuss the numerical solution of the nonlinear Ginzburg-Landau equation for an infinite superconducting thin film with a single circular hole. The results, namely the phase diagram, the jump in the magnetic moment, latent heat, and specific heat are presented in the universal form applicable to any hole radius. Possibilities of measurements of those quantities are also discussed. The conclusions are given in Sec. VI.

## II. NUCLEATION OF SUPERCONDUCTIVITY NEAR A HOLE

Let us consider a thin superconducting film with a single circular hole of a radius  $R$  in a perpendicular magnetic field. This system is analogous to a three-dimensional superconductor with a cylindrical cavity in an axial field if the Ginzburg-Landau parameter  $\kappa = \lambda/\xi$  is large, for one can neglect the screening effect (here  $\lambda$  is the magnetic penetration depth and  $\xi$  is the coherence length). We start with the Ginzburg-Landau (GL) free energy (see, for example Ref. 9):

$$F = \int \left[ a|\Psi|^2 + \frac{b}{2}|\Psi|^4 + \frac{1}{4m} \left| \left[ -i\hbar\nabla - \frac{2e}{c} \mathbf{A} \right] \Psi \right|^2 \right] dV, \quad (1)$$

where as usual  $a = \alpha(T - T_0)$ . More precisely,  $F$  is the difference of the free energy in the superconducting and normal states. For type-II superconductivity (which is always the case for thin films) the screening effect is weak and we may take for the vector potential in (1)  $\mathbf{A} = \frac{1}{2} \mathbf{H} \times \mathbf{r}$ , the vector-potential of the uniform external field  $\mathbf{H}$ . The magnetic-field energy is neglected in (1) for the same reason (in the case of a thin film with thickness  $d$  the screening effect is negligible if  $\kappa_{\text{eff}} = \lambda_{\text{eff}}/\xi = \lambda^2/\xi d \gg 1$  where  $\lambda_{\text{eff}}$  is the effective screening length for a thin film<sup>9</sup>). In our case it is natural to use polar coordinates  $(\rho, \varphi)$  with the origin at the hole center. The equation for the superconducting order parameter is

$$\frac{d^2\psi}{dx^2} + \frac{1}{x} \frac{d\psi}{dx} - \left[ \frac{i}{x} \frac{\partial}{\partial \varphi} + \frac{\phi}{\phi_0} x \right]^2 \psi + \frac{R^2}{\xi^2} (\psi - \psi^3) = 0, \quad (2)$$

where  $\psi = \Psi/\Psi_{\text{GL}}$ ,  $\Psi_{\text{GL}} = \sqrt{|a|/b}$ , order parameter in zero magnetic field at a given temperature, the coherence length  $\xi^2 \equiv \xi^2(T) = \hbar^2/4m|a|$ ,  $T_0$  is the critical temperature in zero field which is the same for uniform and perforated films. Dimensionless coordinate  $x = \rho/R$  is used,  $\phi = \pi R^2 H$  is the flux of the external field through the hole, and  $\phi_0 = \pi \hbar c/e$  is the flux quantum. Here and below we use the dimensionless universal parameters  $R^2/\xi^2(T) = R^2/\xi^2(0)[(T_0 - T)/T_0]$  and  $\phi/\phi_0$  to characterize, respectively, the temperature ( $T$ ) and the magnetic field.

To obtain the upper critical field  $H_{c3}^*(T)$  for the onset of localized superconductivity it is necessary to find a solution of the linearized equation (2) with the following boundary conditions:

$$\left. \frac{d\psi}{dx} \right|_{x=1} = 0 \quad \text{and} \quad \psi(\infty) = 0. \quad (3)$$

To calculate  $H_{c3}^*$  it is enough to seek the solution of (2) in the form

$$\psi_n(x, \varphi) = f_n(x) \exp(in\varphi) \quad (4)$$

with some definite orbital momentum  $n$  (state  $LS_n$ ). Then with the help of a variational method one can find the os-

cillatory dependence  $H_{c3}^*(T)$  directly.<sup>1</sup> The linearized equation (2) can be reduced to Kummer's equation<sup>10</sup> and the exact solutions<sup>2</sup> (see, also, Ref. 11) can be expressed in terms of the confluent hypergeometric functions:

$$f_n(x) = x^n \exp \left[ -\frac{1}{2} \frac{\phi}{\phi_0} x^2 \right] U \left[ Y, n+1, \frac{\phi}{\phi_0} x^2 \right], \quad (4')$$

where

$$U(Y, n, z) = z^{-Y} {}_2F_0 \left[ Y, 1+Y-n; ; -\frac{1}{z} \right]$$

and

$$Y = \frac{1}{2} - \frac{1}{4} \frac{R^2}{\xi^2} \frac{\phi_0}{\phi}.$$

The dependence of  $R^2/\xi^2$  on  $n$  and  $\phi/\phi_0$  can be found solving numerically the equation for the first boundary condition (3) with the function  $f_n(x)$  in form of (4'). The minimum of the ratio  $R^2/\xi^2$  gives us the critical temperature  $T_c^* \equiv T(H_{c3}^*)$ :

$$1 - \frac{T_c^*}{T_0} = \frac{\xi^2(0)}{R^2} \min \left[ \frac{R^2}{\xi^2} \right]$$

(for details, see Ref. 2). Oscillations in  $T_c^*(H)$  (see Fig. 1, thin solid line with cusps) are due to the fact that at different values of the flux this minimum corresponds to different values of the orbital momentum  $n$ .

Such behavior has been observed in experiments with a thin aluminum film of a thickness 800 Å with a lattice of

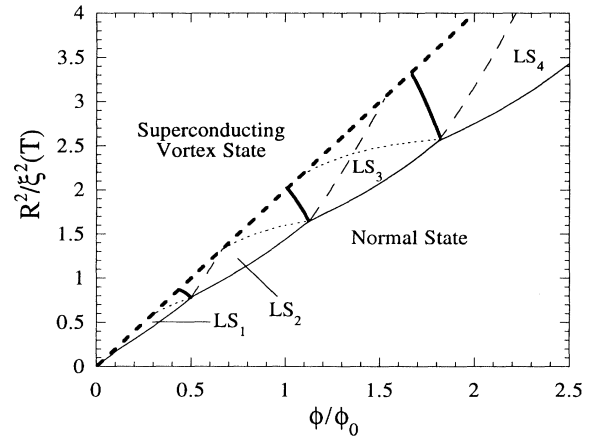


FIG. 1. Phase diagram of a thin film with a single circular hole (of radius  $R$ ) in a perpendicular magnetic field. Here the thin solid curve (with cusps) shows the transitions from the normal state to the localized superconducting states ( $LS_n$ ) characterized by some orbital momentum  $n$ . Thick solid lines are transitions of first order between states with different  $n$ . The curves of absolute instability are shown by thin dashed lines (for the transitions  $n \rightarrow n+1$ ; "superheating" lines) and by dotted lines (for the transitions  $n \rightarrow n-1$ ; "supercooling" lines). The phase diagram is restricted by the thick dashed line which corresponds to the nucleation of a nonzero order parameter everywhere in the film.

circular holes (the hole radius was about  $4 \mu\text{m}$  and the distance between them about  $9 \mu\text{m}$ ).<sup>2</sup> In this work the resistance of the perforated film was measured as a function of the temperature at different values of the external, perpendicular to the film magnetic field ( $H$ ). It was found that while at  $H=0$  the sample exhibits a single sharp resistive transition, it splits into two steps in nonzero fields. In accordance with this, one can introduce two critical temperatures corresponding to the first and the second drops of the resistance.

At the upper critical temperature ( $T_c^*$ ) the superconductivity appears near the holes in accordance with the previous discussion and the resistance decreases by some factor which depends on the relation between the coherence length and the distance between the holes. In principle, such a state of localized superconductivity can have zero resistance if the separation between the holes is smaller or of the order of the coherence length. Experimentally a good agreement was found between the calculated (Fig. 1, thin solid line) and measured critical temperature at high enough magnetic field when the coher-

ence length at  $T_c^*$  is small and the holes can be considered as independent. On the contrary, a number of collective effects was observed at weak fields, for instance a new type of oscillation in the  $T_c^*(H)$  with the period corresponding to one flux quantum through a unit cell of the square lattice of holes. At the lower critical temperature, which coincides with the critical temperature of a reference uniform film without holes, the resistance of the sample drops to zero.

### III. SOME GENERAL FORMULAS FOR THE REGION BELOW THE CRITICAL TEMPERATURE

To investigate the properties of superconducting states with different orbital momentum  $n$  and in particular to find the line of the phase transition between them (which is of first order as we will see below) the use of the exact solutions of the nonlinear equation (2) is necessary. Then it is possible to compare the free energy of the different states:

$$F = 4F_{\text{disk}} \int_0^{2\pi} \frac{d\varphi}{2\pi} \int_1^\infty x dx \left[ |\psi|^2 - \frac{1}{2} |\psi|^4 - \frac{\xi^2}{R^2} \left| \frac{\partial \psi}{\partial x} \right|^2 - \frac{\xi^2}{R^2} \left| \left[ \frac{i}{x} \frac{\partial}{\partial \varphi} + \frac{\phi}{\phi_0} x \right] \psi \right|^2 \right], \quad (5)$$

where  $F_{\text{disk}} = -\pi R^2 d (a^2/2b)$  is the GL free energy of a superconducting disk with the radius  $R$  and thickness  $d$  in zero magnetic field.

From (5) one can derive the magnetic moment  $M_n = -\partial F_n / \partial H$  in the state  $S_n$  with orbital momentum  $n$ :

$$M_n = \tilde{M} \int_1^\infty x^2 f_n^2(x) \left[ \frac{n}{x} - \frac{\phi}{\phi_0} x \right] dx, \quad (6)$$

where

$$\tilde{M} = \frac{\phi_0}{(2\pi\lambda)^2} \pi R^2 d$$

and

$$\lambda^{-2} = \frac{8\pi e^2 \Psi_{\text{GL}}^2}{mc^2},$$

the entropy

$$S_n = -\frac{\partial F_n}{\partial T} = 2S_{\text{disk}} \int_1^\infty f_n^2 x dx, \quad (6')$$

where  $S_{\text{disk}} = -(\partial a / \partial T) \Psi_{\text{GL}}^2 \pi R^2 d$  is the entropy of a superconducting disk of radius  $R$  and thickness  $d$  in zero field, the latent heat

$$\Delta Q[n \rightarrow n+1] = T(S_n - S_{n+1}), \quad (6'')$$

and at last the specific heat

$$\frac{C_n}{C_{\text{disk}}} = 2 \int_1^\infty f_n^2 x dx + 2\tau \frac{\partial}{\partial \tau} \left[ \int_1^\infty f_n^2 x dx \right], \quad (6''')$$

where  $\tau = R^2 / \xi^2(T)$  and  $C_{\text{disk}} = T/b(\partial a / \partial T)^2 \pi R^2 d$  is

the specific heat of the superconducting disk of radius  $R$  and thickness  $d$  in zero field. Under all these quantities we understand the difference between superconducting and normal states at a given temperature.

### IV. TRANSITIONS OF THE TYPE $S_n \rightarrow S_{n+1}$ BETWEEN SUPERCONDUCTING STATES WITH DIFFERENT ORBITAL MOMENTA: LITTLE-PARKS GEOMETRY

Before proceeding further let us consider the transition between states with different orbital momentum  $n$  for the simplest geometry:<sup>3</sup> a thin-wire superconducting loop of radius  $R$  and wire thickness  $D \ll R$ , ( $\lambda \gg \xi \gg D$ ) in a magnetic field parallel to its axis. The system under consideration is exactly equivalent to a thin-walled cylinder in an axial magnetic field—the original Little-Parks geometry. In such a case the superconducting order parameter depends on the polar angle  $\varphi$  only and the free energy may be written simply

$$F_{\text{LP}} = -\frac{\pi^2}{2} R D^2 \frac{a^2}{b} \int_0^{2\pi} \left[ |\psi|^2 - \frac{1}{2} |\psi|^4 - \frac{\xi^2}{R^2} \left| \left[ i \frac{\partial}{\partial \varphi} + \frac{\phi}{\phi_0} \right] \psi \right|^2 \right] \frac{d\varphi}{2\pi}. \quad (7)$$

The transition temperature to the state  $S_n$ :  $\psi_n = f_n \exp(in\varphi)$  is immediately obtained from (7) in quadratic (over  $\psi$ ) approximation

$$\frac{R^2}{\xi^2} = \left[ \frac{\phi}{\phi_0} - n \right]^2. \quad (8)$$

The orbital momentum which corresponds to the minimum of  $R^2/\xi^2$  gives a transition temperature which is an oscillatory dependence of the magnetic field (see Fig. 2, thin solid line). It is the usual Little-Parks effect.<sup>3</sup> To find the line of the first-order transition between the  $n$  and  $n+1$  states below the critical temperature we must compare the exact expression (7) for the corresponding free energies. It gives the vertical lines  $\phi/\phi_0 = n + 1/2$  on the  $H$ - $T$  plane in Fig. 2, i.e., the transition field is temperature independent in the Ginzburg-Landau approximation.

The line of absolute instability ("superheating" boundary) of the  $n$  state may be easily obtained by looking at the change of the energy of the  $n$  state due to admixture of  $n+1$ -state:

$$\psi = f_n \exp(in\varphi) + \eta f_{n+1} \exp[i(n+1)\varphi]. \quad (9)$$

In the Little-Peaks case,  $f_n$  and  $f_{n+1}$  are independent of the coordinates;  $\eta$  can be considered as a new order parameter which describes a second-order phase transition from the  $n$  state to the state and lower symmetry (9). Now following the usual scheme of type-II transition analysis one can substitute (9) into the free energy (7) and find its expansion with respect to the even powers of  $\eta$ :

$$F_{LP} = F_{LPn} + A\eta^2 + \frac{1}{2}B\eta^4 \quad (10)$$

where

$$F_{LPn} = -\frac{\pi^2}{2}RD^2\frac{a^2}{b} \left\{ f_n^2 \left[ 1 - \frac{1}{2}f_n^2 - \frac{\xi^2}{R^2} \left( \frac{\phi}{\phi_0} - n \right)^2 \right] \right\}, \quad (10')$$

$$A = -\frac{\pi^2}{2}RD^2\frac{a^2}{b} \left\{ f_{n+1}^2 \left[ 1 - 2f_n^2 - \frac{\xi^2}{R^2} \left( \frac{\phi}{\phi_0} - n - 1 \right)^2 \right] \right\},$$

and

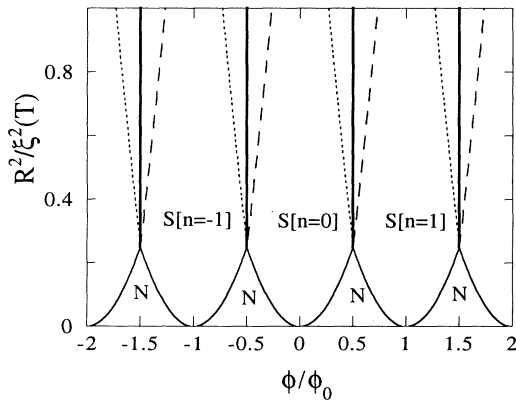


FIG. 2. Phase diagram of a thin-wire loop.  $N$ , normal state;  $S[n]$ , superconducting state with the orbital momentum equal  $n$ . Thick solid lines show the first-order phase boundaries between the states with different  $n$ . The dashed and dotted curves are the lines of absolute instability ("superheating" and "supercooling" boundaries).

$$B = \frac{\pi^2}{2}RD^2\frac{a^2}{b}f_{n+1}^4$$

The transition from the  $n$  state to the hybrid state (9) starts to be energetically favorable when the coefficient  $A$  before  $\eta^2$  changes sign (from positive to negative). The condition  $A=0$  [which as it is clear from (10') is independent of the amplitude  $f_{n+1}$ ] gives us the line of absolute instability of the  $n$  state with respect to the transition to the  $n+1$  state (Fig. 2, dashed lines):

$$\frac{R^2}{\xi^2} = \left( \frac{\phi}{\phi_0} - (n-1) \right)^2 - 2. \quad (11)$$

As it is clear from Fig. 2, the lines (11) are just "superheating" lines but do not correspond to any thermodynamic transition because the first-order transition from the pure  $n$  state to the pure  $n+1$ -state always (in thermodynamically equilibrium cases) takes place earlier in the field. The "overcooling" lines (dotted curves in Fig. 2) or the lines of the  $n$ -state instability with respect to the  $n-1$  state take place always at lower field than the corresponding first-order transition and can be expressed as

$$\frac{R^2}{\xi^2} = \left( \frac{\phi}{\phi_0} - (n+1) \right)^2 - 2.$$

## V. PHASE DIAGRAM AND $LS_n \rightarrow LS_{n+1}$ TRANSITIONS IN A FILM WITH A HOLE

The case of a hole (radius  $R$ ) in a film (thickness  $d$ ) in perpendicular magnetic field  $H$  is more complicated than a thin-wire loop because now the factor  $f_n$  in (4) is a function of the dimensionless polar radius  $x = \rho/R$ . To calculate the free energy we need to know the spatial distribution of the order parameter in the film. The nonlinear Eq. (2) can be solved numerically taking the order parameter in the form (4) (to make the equation be one dimensional) and using the boundary conditions (3). Below the critical field  $H_{c3}^*(T)$  there is one nonzero value of the order parameter at the hole edge (starting value)  $f_{n0} > 0$  which is consistent with the second condition of (3) (the first boundary condition, namely zero derivative of the order parameter at  $x=1$  is fulfilled in all cases). If one takes  $f_n(1) > f_{n0}$  then the numerical solution  $f_n(x)$  is always positive and infinite when  $x$  approaches infinity. In the opposite case when  $f_n(1) < f_{n0}$ ,  $f_n(x)$  approaches negative infinity at large  $x$ . Above the critical field  $H_{c3}^*$  one can satisfy the second condition (3) only if  $f_n(1) = 0$ , i.e., there is no nontrivial solution.

In Fig. 3 one can see the evolution of the order parameter localized near the hole (state  $LS_4$ ) with decreasing magnetic field at a constant temperature. The dashed curves correspond to  $H < H_{c2}$  or in other words to  $\phi/\phi_0 < (1/2)(R^2/\xi^2)$ . Similar to the case of a plane surface in parallel field<sup>12</sup> we find that if the field is small enough (for given  $n$ ) then the maximum of  $f$  is shifted from the hole edge. For example if one follows the critical temperature line  $T(H_{c3}^*)$  ( $N$ - $S$  boundary in Fig. 1) then

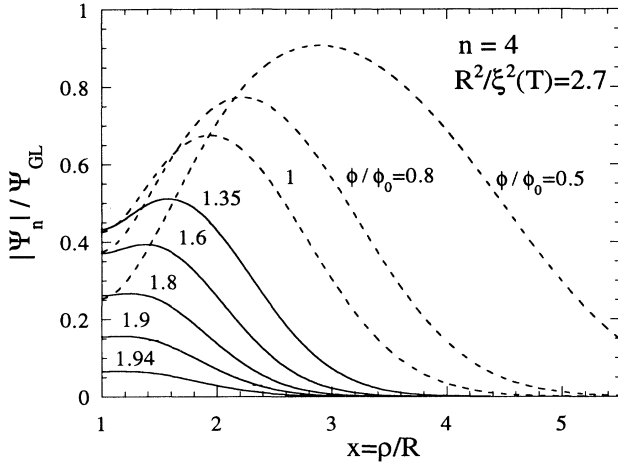


FIG. 3. Spatial distribution of the dimensionless order parameter normalized to  $\Psi_{GL}(T)$ , the value of the order parameter at the same temperature but at  $H=0$ . The temperature is given by the relation:  $R^2/\xi^2(T)=2.7$ ,  $\rho$  is the distance to the hole center and  $R$  is the hole radius. Dashed curves correspond to fields smaller than  $H_{c2}$ .

in the left vicinity of each cusp the maximum of the order parameter coincides with the hole edge [ $x(f_{\max})=1$ ], while when the field is slightly higher than the cusp field the maximum is shifted [ $x(f_{\max})>1$ ]. When the state  $LS_n$  has the maximum critical temperature with respect to the  $LS_{n+1}$  and  $LS_{n-1}$  and  $H > H_{c2}$  the shift is of the order of  $\xi$  or smaller (at  $H=H_{c2}$  the  $\xi \approx 0.6R$  in Fig. 3). Similar to Ref. 12 no abrupt change in the order-parameter distribution was observed at  $H=H_{c2}$ . In this paper we consider only the region  $H > H_{c2}$  because below  $H_{c2}$  the second boundary condition (3) is not true and our approach is not valid.

After  $f(x)$  is calculated one can easily find the first-order transition lines [using (4) and (5) and the condition  $F_{n+1}=F_n$ ] between the states with different orbital momentum  $n$  (Fig. 1, thick solid lines). The transition from the normal into the superconducting states in Fig. 1 is shown by the thin solid line. It is a second-order transition which is calculated from the linearized GL equation<sup>1</sup> (see, also, Ref. 2). The diagram is restricted by the thick dashed line which represents the appearance of the nonlocalized superconducting (mixed) state everywhere in the film.

As in the case of the hollow cylinder [see Eqs. (10) and (10')] the lines of absolute instability were calculated by the substitution of (4) [where  $f_{n+1}$  was the solution of the linearized equation (2)] into (5) and looking for the temperature (at fixed magnetic field) when the coefficient before  $\eta^2$  starts to be negative. In Fig. 1 the thin dashed lines are the "superheating" lines corresponding to the transitions of the type " $n \rightarrow n+1$ " in increasing field (and fixed temperature). The  $n$  state cannot exist when the field is higher than the "superheating" field and the system must jump into the  $n+1$  state. The "supercooling" boundaries are shown by dotted curves.

Knowledge of the order parameter enables us to calculate the magnetic moment of our system (6). The field dependence of the magnetic moment calculated for two different temperatures is shown in Fig. 4. Solid curves correspond to the thermodynamic equilibrium (minimum free energy). One can see the jump corresponding to the first-order transition. If the equilibrium is not established the system can follow dashed curves ("superheating" and "supercooling" processes). Only with increasing field (see also phase diagram) the system can reach the instability line. The jump of the magnetic moment at the "superheating" point is of opposite sign with respect to the point of the first-order transition.

Figure 5 shows the jump of the magnetic moment as a function of the magnetic field at the first-order transition  $LS_n \rightarrow LS_{n+1}$ . Corresponding latent heat (6'') is also shown.

Specific heat (6''') of the film with a hole is shown as a function of the temperature in Fig. 6 for some values of the reduced flux through the hole. The first jump in each curve corresponds to the second-order  $N \rightarrow LS_n$  transition. At a lower temperature which corresponds to the first-order transition  $S_n \rightarrow S_{n+1}$ , there is another jump in the specific heat. The infinite singularity corresponds to the latent heat. As it is clear from Fig. 6 the jumps are of the same order of magnitude (or even higher) as the jump of the specific heat at  $T_0$  of the disc (radius  $R$  and thickness  $d$ ) in zero field which is equal to

$$C_{\text{disk}}|_{T=T_0}.$$

To see whether these transitions can be observed experimentally let us estimate the magnetic moment of a perforated film. As an example we consider a thin Nb film

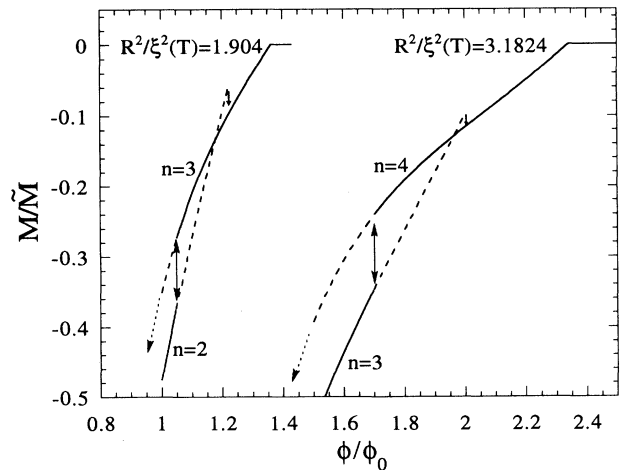


FIG. 4. Magnetic moment of a thin film with a hole in the state of localized superconductivity with orbital momentum  $n$  as a function of the reduced flux through the hole for two values of the temperature. The jumps correspond to first-order transitions between states with different  $n$ . The dashed extrapolations correspond to "superheating" and "supercooling" regions.

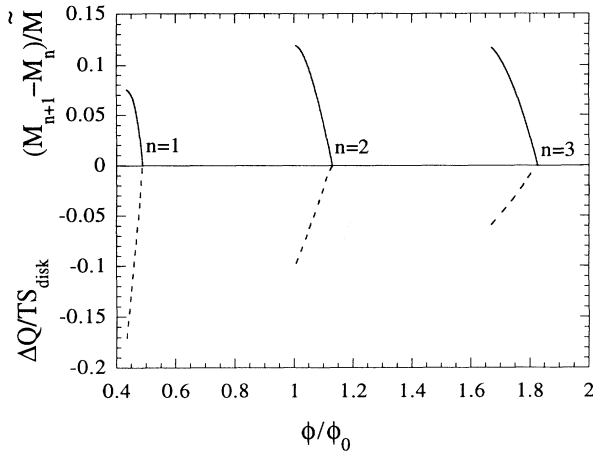


FIG. 5. Values of the magnetic moment jumps and of the latent heat for a thin film with a hole along the first-order phase transition lines which correspond to transitions of the orbital momentum  $n \rightarrow n + 1$  (see thick solid lines in Fig. 1).

of a thickness  $1000 \text{ \AA}$  with 4 000 000 holes of a diameter  $1 \mu\text{m}$  which form a square lattice with a period  $5 \mu\text{m}$ . In such a case the holes are separated enough to be independent [coherence length is of the order of the hole radius or smaller along the lines of first-order transitions (Fig. 1)] and the total area of the sample will be  $1 \text{ cm}^2$ . All the results in Figs. 4 and 5 are presented in units of  $\tilde{M}$  [see Eq. (6)] which can be written in the form  $(\phi_0/4\pi)(R/\xi)^2(d/\kappa^2)$ . For our example this value is equal approximately to  $7 \times 10^{-15} \text{ emu}$ . Here we take into account that  $\kappa \approx 5$  and for transitions between small  $n$  one can take  $\xi \approx R$  (in general case  $R/\xi \geq 0.88$  on the first-order transition lines). The jump in the magnetic moment is approximately, by a factor of 10, smaller than  $\tilde{M}$  (Figs. 4 and 5) so the total jump for the array of  $4 \times 10^6$  holes will be about  $3 \times 10^{-9} \text{ emu}$ . Such value can be observed experimentally. As an example of similar measurements one can consider Ref. 11 (and references there), where the magnetization of an array of thin disks was measured with the accuracy  $10^{-10} \text{ emu}$ . A multilayer system can be used to increase the signal.

The specific heat of the same Nb perforated film can be also easily found. The total jump in the specific heat is equal approximately to the  $\Delta C = 6NC_{\text{disk}} = 6 \times 10^{-8} \text{ J/K}$  [ $N$  is the total number of holes; see (6''') and Fig. 6 for the relation between the specific heat of the disk in zero field and of the hole]. We take for the specific-heat jump in Nb at zero field the value  $0.036 \text{ J/K cm}^3$ . Note that in this paper we assume under the specific heat the difference between the specific heat in the normal and in the superconducting states. The calculated magnitude for  $\Delta C$  can be observed experimentally as one can understand from Ref. 13 where a new calorimeter for thin-film applications is presented. The addenda of the device is equal to  $2 \times 10^{-9} \text{ J/K}$  at  $4.3 \text{ K}$ .

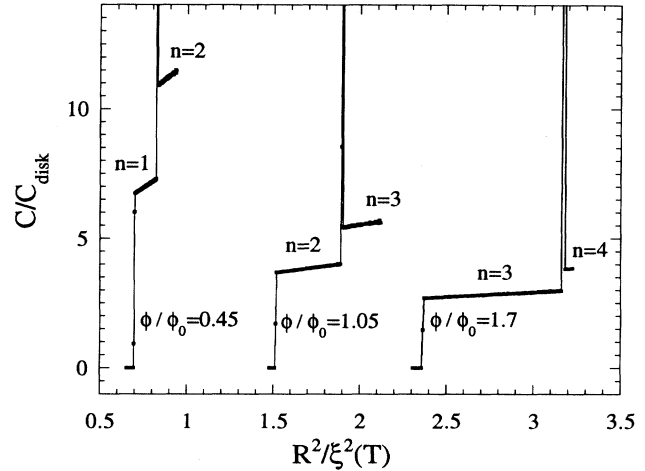


FIG. 6. Dimensionless specific heat of a thin film with a circular hole at three values of the magnetic field as a function of the dimensionless temperature:  $R^2/\xi^2(T) = R^2/\xi^2(0)(T_0 - T)/T_0$ . The first jump corresponds to the second-order transition from the normal to the localized superconducting state while the second one with an infinite peak represents the first-order transition of the type  $n \rightarrow n + 1$ . Here  $C_{\text{disk}}$  is the specific heat of the thin disk of radius  $R$  and thickness  $d$  in zero field.

## VI. CONCLUSION

A numerical solution of the nonlinear Ginzburg-Landau equation is used to reconstruct the phase diagram of a thin superconducting film with a single circular hole. The results are presented in Fig. 1 in the universal form. Our calculations are valid only if the field is higher than the bulk upper critical field  $H_{c2}$ , i.e., when a nonzero order parameter exists only near the hole edge due to the effect of surface superconductivity.<sup>14,12</sup> In accordance to this we restrict the phase diagram by the thick dashed line which represents the second-order transition into the Abrikosov vortex state.

The phase diagram of the thin-wire loop (Little-Parks geometry) has been found analytically (Fig. 2). In both cases the transitions between different superconducting  $n$  states were shown to be of first order. Corresponding jumps in the magnetic moment and latent heat are calculated. While in the case of the circular wire loop the boundaries between the states with different orbital momentum are parallel to the temperature axis, it is not the case for a perforated film. In the last case, first-order transition can be observed under decreasing the temperature at constant field. It can be easily shown that one may neglect the screening effect for a superconducting film (as we do here) assuming that  $\lambda_{\text{eff}} \gg \xi$  ( $d < \xi$  in our consideration).

Two systems considered in this paper are exactly equivalent to the corresponding three-dimensional (3D) configurations: a thin-walled hollow cylinder and a cylin-

dricial cavity in a bulk superconductor if the screening effect can be neglected. The last example is realized in high- $T_c$  superconductors with columnar defects. The screening effect in the 3D geometry can be neglected if  $\kappa^2 = \lambda^2 / \xi^2 \gg 1$ , which is usually the case in high- $T_c$  superconductors ( $\kappa \sim 100$ ).

For experimental observation we suggest using artificially prepared thin films with an array of holes. The magnitudes of the specific heat and of the magnetization jump are estimated and are shown to be measurable.

#### ACKNOWLEDGMENTS

We are grateful to J.-P. Brison for a careful reading of the manuscript and useful remarks. One of the authors (A. Bezryadin) would like to express his acknowledgment to A. Zheludev for many clarifying discussions. We are also grateful to Yu.N. Ovchinnikov who called our attention (after the paper was ready for publication) to Ref. 15 where he considered theoretically the nucleation of superconductivity in a cylinder and near a cylindrical cavity.

---

\*Also at the Center for Condensed Matter Theory, P.O. Box 55, Moscow 109518, Russia.

<sup>1</sup>A. Buzdin, Phys. Rev. B **47**, 11 416 (1993).

<sup>2</sup>A. Bezryadin and B. Pannetier, J. Low Temp. Phys. (to be published).

<sup>3</sup>W. A. Little and R. D. Parks, Phys. Rev. Lett. **9**, 9 (1962); Phys. Rev. A **133**, 97 (1964).

<sup>4</sup>W. Gerhauser *et al.*, Phys. Rev. Lett. **68**, 879 (1992).

<sup>5</sup>L. Civale *et al.*, Phys. Rev. Lett. **67**, 648 (1991).

<sup>6</sup>H. J. Fink and V. Grunfeld, Phys. Rev. B **22**, 2289 (1980).

<sup>7</sup>H. Fink, A. Lopez, and R. Maynard, Phys. Rev. B **26**, 5327 (1982).

<sup>8</sup>B. Pannetier, in *Quantum Coherence of Mesoscopic Systems*, Vol. 254 of *Nato Advanced Study Institute, Series B: Physics*,

edited by B. Kramer (Plenum, New York, 1991).

<sup>9</sup>A. A. Abrikosov, *Fundamentals of Theory of Metals* (North-Holland, Amsterdam, 1988).

<sup>10</sup>*Handbook of Mathematical Functions*, edited by M. Abramowitz and I. A. Stegun (Dover, New York, 1970), p. 504.

<sup>11</sup>O. Buisson, P. Gandit, R. Rammal, Y. Y. Wang, and B. Pannetier, Phys. Lett. A **150**, 36 (1990); R. Rammal (unpublished).

<sup>12</sup>H. J. Fink, Phys. Rev. Lett. **14**, 309 (1965).

<sup>13</sup>D. W. Denlinger *et al.*, Rev. Sci. Instrum. **65**, 946 (1994).

<sup>14</sup>D. Saint-James and P. G. de Gennes, Phys. Lett. **7**, 306 (1963).

<sup>15</sup>Yu.N. Ovchinnikov, Sov. Phys. JETP **52**, 755 (1980).